Available online at www.sciencedirect.com
SCIENCE DIRECT®
ELSEVIER
Nuclear Instruments and Methods in Physics Research B 206 (2003) 254–258
NIM B
Beam Interactions with Materials & Atoms
www.elsevier.com/locate/nimb

Fluorine-doping in titanium dioxide by ion implantation technique

T. Yamaki [a,*], T. Umebayashi [b], T. Sumita [c], S. Yamamoto [a], M. Maekawa [a], A. Kawasuso [a], H. Itoh [a]

[a] *Department of Materials Development, Takasaki Radiation Chemistry Research Establishment, Japan Atomic Energy Research Institute, 1233 Watanuki, Takasaki, Gunma 370-1292, Japan*

[b] *Department of Quantum Engineering and Systems Science, Graduate School of Engineering, The University of Tokyo, 7-3-1 Hongo, Bunkyo-ku, Tokyo 113-8656, Japan*

[c] *Technology Research Department, National Space Development Agency of Japan, 2-1-1, Sengen, Tsukuba, Ibaraki 305-8505, Japan*

Abstract

We implanted 200 keV F^+ in single crystalline titanium dioxide (TiO_2) rutile at a nominal fluence of 1×10^{16} to 1×10^{17} ions cm^{-2} and then thermally annealed the implanted sample in air. The radiation damage and its recovery process during the annealing were analyzed by Rutherford backscattering spectrometry in channeling geometry and variable-energy positron annihilation spectroscopy. The lattice disorder was completely recovered at 1200 °C by the migration of point defects to the surface. According to secondary ion mass spectrometry analysis, the F depth profile was shifted to a shallower region along with the damage recovery and this resulted in the formation of an F-doped layer where the impurity concentration steadily increased toward the surface. The F doping proved to provide a modification to the conduction-band edge of TiO_2, as assessed by theoretical band calculations.

PACS: 61.72.–y; 61.80.Jh; 71.55.–i; 85.40.Ry
Keywords: Titanium dioxide (TiO_2); Ion implantation; Anion doping; RBS/channeling; Positron annihilation; Electronic structure

1. Introduction

Titanium dioxide (TiO_2) is a functional material with photocatalysis and photoconductivity characteristics that provide various technological applications [1]. In most studies concerning such electrochemical properties of TiO_2, it is of great interest to improve the separation of the photogenerated electron–hole pairs or to extend the wavelength range of the TiO_2 photoresponses into the visible region. To solve these problems, doping TiO_2 with different transition-metal ions has been intensively carried out using ion implantation. Anpo et al. [2] described a Cr- or V-doped TiO_2 photocatalyst prepared by this technique. Their study suggests that the ion implantation provides an effective modification of the photocatalytic material's electronic structures.

* Corresponding author. Tel.: +81-27-346-9413; fax: +81-27-346-9687.
E-mail address: tetsuya@taka.jaeri.go.jp (T. Yamaki).

0168-583X/03/$ - see front matter
doi:10.1016/S0168-583X(03)00735-3

In contrast to these studies on the metal-ion implantation, there were only a few reports on the use of anionic species for doping. Quite recently, however, anion doping has been receiving much attention as a method for controlling the optical properties of TiO_2 since a nitrogen-doping study [3]. We independently focused on fluorine (F) doping into TiO_2 to modify its electronic structures. The fluorination of TiO_2 surfaces would enhance their chemical and optical stabilities and so F ions have the possibilities of acting as promising dopants in a TiO_2 photocatalyst.

Our preliminary experiments [4] demonstrated for the first time that the F ion implantation and subsequent thermal treatment made it possible to prepare an F-doped TiO_2 layer. However, further investigations to reveal the details about damage recovery and impurity diffusion are required for a better understanding of the implantation effect. In this study, we investigated the annealing behavior of TiO_2 implanted with F ions based on two different techniques, Rutherford backscattering and channeling (RBS-C) and variable-energy positron annihilation measurements. The electronic structures of the F-doped TiO_2 were also analyzed by the theoretical band calculations to predict the doping effect on the spectral response of TiO_2.

2. Experimental

Optically polished single-crystalline TiO_2 (rutile) with a $\langle 0\,0\,1\rangle$ crystallographic axis was used for our experiments. The size was about 10×10 mm^2 in area and 0.5 mm in thickness. The ion implantations were performed at room temperature with 200 keV F^+ ions at a nominal fluence of 1×10^{16} to 1×10^{17} ions cm^{-2}. The mean projected range, R_p, and range straggling, ΔR_p, were calculated to be 274 and 72 nm, respectively, by the TRIM code [5]. The displacement energies of 50 eV for both Ti and O atoms [6] were used for evaluating the damage distributions. After the implantation, an isochronal annealing was carried out in air up to 1200 °C for 5 h for each step.

Helium ions of 2.0 MeV were generated by a 3 MV single-ended accelerator and utilized for the RBS-C measurements. A positron beam with energies of 0.2–25 keV was used to measure the Doppler broadening (characterized by the so-called S parameter) of electron–positron annihilation γ rays at room temperature. We estimated an experimental error in the S-parameter analysis based on the general law of statistical uncertainty. X-ray photoelectron spectroscopy (XPS) measurements with a Mg X-ray source ($K\alpha = 1253.6$ eV) confirmed the occupation of F atoms on O-lattice sites in the outermost region of the implanted surface layer [4]. Secondary ion mass spectrometry (SIMS) analysis was employed for probing the as-implanted and postanneal F distributions. The electronic structures of the F-doped TiO_2 were calculated by the full-potential linearlized augmented plane wave (FLAPW) formalism [7] in the framework of the generalized gradient approximation (GGA) [8,9].

3. Results and discussion

Fig. 1 shows the typical RBS-C spectra for the TiO_2 single crystal implanted with a dose of 9×10^{16} ions cm^{-2} and then isochronally annealed for 5 h for each step. It is clearly seen in the

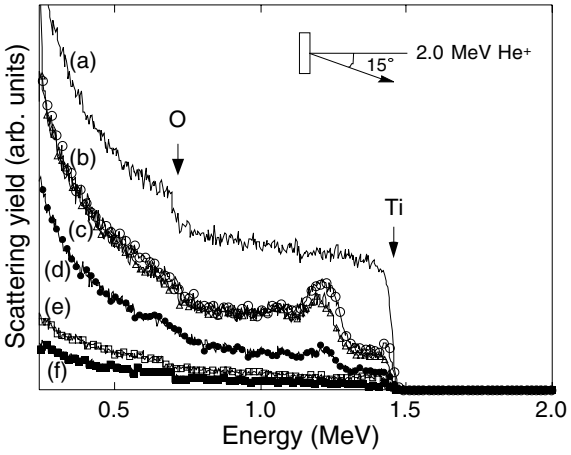

Fig. 1. 2.0 MeV $^4He^+$ (a) random and $\langle 0\,0\,1\rangle$ aligned RBS spectra of the TiO_2 rutile single crystal implanted with 200 keV F^+ (9×10^{16} ions cm^{-2}) at room temperature, for the as-implanted sample (b) and after annealing in air at (c) 300, (d) 600, (e) 1000 and (f) 1200 °C. Arrows indicate each constituent element existing on the sample surface.

as-implanted state that the surface peak was well separated from the damaged peak near the R_p for the Ti sublattice. This observation is in agreement with previous results regarding the damage formation and accumulation in metal-ion implanted TiO_2 [10]. Both peaks did not reach the heights of the random levels, indicating that the dose for the implantation corresponding to 8 dpa (displacements per atom) was insufficient to render TiO_2 completely channeling amorphous.

The lowering of the disorder peak height was observed during the course of isochronal thermal treatment. This can be attributed to a columnar regrowth within the total thickness of the damaged layer [10]. The pronounced recovery in the Ti and O sublattices was achieved by such a recrystallization process up to the highest annealing temperature of 1200 °C. The minimum yield, χ_{min}, the random-to-aligned ratio of backscattering yields, gives a measure of the degree of lattice disorder in crystalline solids. For the Ti sublattice, we obtained a χ_{min} value of 4% near the surface where the dechanneling contribution to the yields is the smallest.

Fig. 2 displays a plot of the S parameter versus the incident positron energy (hereafter referred to as S versus E) for the TiO_2 single crystal implanted with 9×10^{16} F^+ ions cm^{-2} and the samples after the 5 h isochronal annealing. Data for a virgin (unimplanted) TiO_2 substrate are also exhibited in the figure as a reference. The upper horizontal axis shows the mean positron implantation depth given by an empirical formula [11]. The positron diffusion length is determined to be 42 nm by fitting the S versus E data for the virgin sample based on the VEPFIT program [12]. For the as-implanted sample, the S parameters became much greater than that in the virgin state at every positron energy except for the bulk region around $E = 25$ keV. This result indicates that vacancy-type defects, which trap positrons, were introduced by the F implantation.

The thermal treatment at 300 °C led to no changes in the S versus E plot, suggesting that the disorder phase is stable, although the above RBS data showed that the damaged recovery appeared to start at this temperature. During the annealing stages at 600 and 1000 °C, the S value decreased at

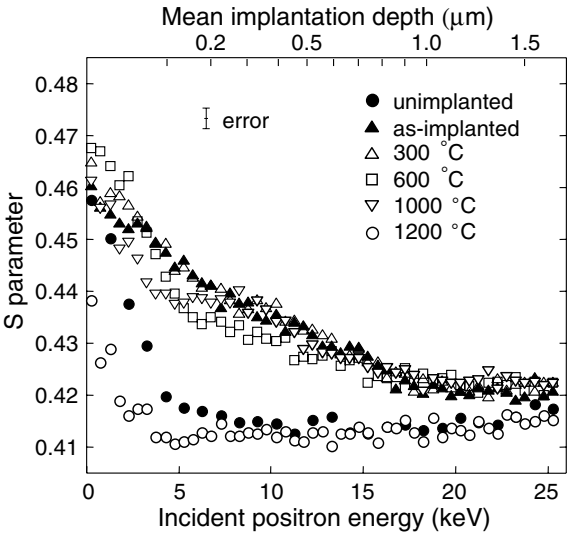

Fig. 2. The S parameter versus positron incident energy for the samples implanted with 9×10^{16} F ions cm^{-2} at room temperature, after the implantation and upon 5 h isochronal annealing. The upper horizontal axis represents the mean implantation depth of the positrons. An error bar (± standard deviation) for the S parameter is also provided in this figure.

$4 < E < 15$ keV and increased in the lower energy region ($E < 4$ keV). This means that the vacancy migration to the surface, acting as a sink of point defects, occurred along with the damage recovery. Almost all vacancy-type defects were annealed out at 1200 °C. A reduction in the S parameter from the virgin sample level is possibly due to a certain change in the surface state induced by the thermal treatment, rather than by the impurity doping, since the virgin sample showed the same result after the annealing.

As we described elsewhere [4], the substitution of the F atoms for O-lattice sites, i.e. the formation of $TiO_{2-x}F_x$ was confirmed by the XPS results obtained after complete annealing. In line with our previous paper, the XPS data were also used for a quantitative estimation of the atomic ratio of F to O, F/O. For the sample implanted with 9×10^{16} F^+ ions cm^{-2}, the F/O ratio was calculated to be 0.0065, which means the formation of $TiO_{2-x}F_x$ compounds with $x = 0.013$ if F has a substitutional fraction of $f_s = 1$. Such high substitutional fractions of F in a TiO_2 host (especially at low concentrations as in our case) can be reasonably

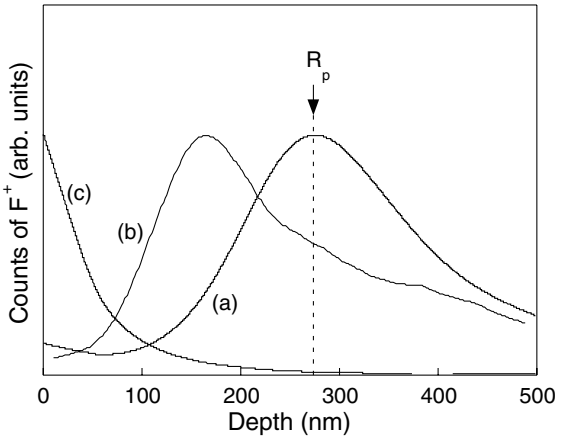

Fig. 3. SIMS F depth profiles of 200 keV F^+-implanted TiO_2 rutile single crystal (a) before and after the thermal treatments at (b) 600 and (c) 1200 °C. The F^+ secondary ion counts plotted as the ordinate are normalized in such a way that the maximum of both profiles is equal. For comparison, the calculated value of R_p is also shown in this figure.

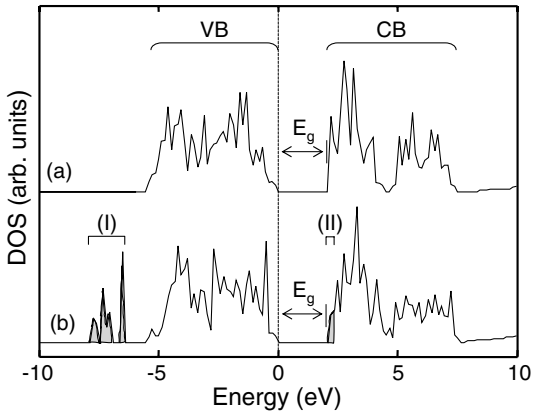

Fig. 4. Total DOSs of (a) pure and (b) F-doped TiO_2 calculated by FLAPW. The dopant F is located at the substitutional site for an O atom in the rutile TiO_2 crystal (the two TiO_2 unit cells). The energy on the horizontal axis is measured from the top of the VBs. E_g indicates the (effective) bandgap energy of the semiconductors. The impurity states are labeled (I) and (II).

predicted by the consideration based on the solubility rules for equilibrium and ion-implanted solid solutions [13], as well as by the experimental results from previous studies [10].

In Fig. 3, the SIMS F depth profiles of the implanted rutile single crystals are compared between before and after the isochronal annealing. Note that there should be a possible evaporation of F as a volatile component from the TiO_2 surface during the thermal treatment. The profile for the as-implanted sample had a peak located at 270–280 nm, which is very close to the calculated value of R_p (see above). During the course of the annealing, it appears that a significant amount of implanted atoms diffused to the outer surface. After the annealing at 1200 °C, this led to the formation of a new phase where the impurity concentration steadily increased toward the surface. Such an impurity migration was recently observed for implanted SiC [14] and InP [15] single crystals. The implication is that grain boundaries or extended defects are created by the implantation, so that the activation enthalpy for the motion of impurity atoms in the lattice effectively decreases. This can induce a preferred outward migration of the F atoms at high temperatures, where the above-mentioned damage recovery progresses.

Fig. 4 provides the total densities of states (DOSs) calculated for pure and F-doped TiO_2. The calculation model had two unit cells of rutile TiO_2, where one F atom is replaced with one O atom. In the pure TiO_2 crystal, the valence and conduction bands (referred to as VB and CB, respectively) consist of both the Ti3d and O2p orbitals. Since the Ti3d orbital is split into two parts, the t_{2g} and e_g states, the CB can be divided into lower and upper bands. When TiO_2 is doped with F, the localized levels with a high density appear below the VB (shown as (I)). These levels are composed of the F2p state without any mixing with the VB or CB and, consequently, they are not expected to contribute to the optical absorption spectra of TiO_2.

The spectral response property of semiconductors is directly affected by their electronic structure *within or near the bandgap*. Therefore, it is important to note that the DOS around the lower edge of the CB is modified by the F doping (labeled as (II)). According to the electron density map of this impurity states projected onto the (1 1 0) lattice plane (not shown), such a change originates from the occurrence of the electron occupied level, which consists of the t_{2g} state of the Ti3d orbital. These results are similar to the

property of the level due to the O vacancy [16]. Nakamura et al. [17] reported that the O vacancies were produced in TiO_2 by a hydrogen plasma treatment. The resulting O deficient TiO_2 showed photocatalytic activity in the visible-light region (up to 600 nm) for nitrogen monoxide removal. Thus the O vacancy can provide good modifications to the TiO_2 band structures. In this sense, it is expected that the substitutional doping of F, like the O vacancy, can reduce the effective bandgap energy of TiO_2, thereby inducing visible-light photoresponses. Actually, the DOS of Fig. 4(b) seems to have a tail of donor-like states into the bandgap below the CB.

4. Conclusions

We demonstrated the effects of F implantation in TiO_2 rutile single crystals followed by thermal annealing. The isochronal annealing processes at 300, 600, 1000 and 1200 °C for 5 h for each step led to the formation of an F-doped TiO_2, i.e. the $TiO_{2-x}F_x$ phase, along with the recovery of the radiation damage. The disorder layer was recovered by the surface migration of vacancy-type defects and, simultaneously, implanted F atoms diffused to the outer surface. The resulting doped phase showed a new concentration gradient; the concentration increases with decreasing depths into the surface. From the theoretical band calculations using the FLAPW method, it was found that the F doping gave rise to a modification of the electronic structure around the CB edge of TiO_2. This probably leads to a reduction in the effective bandgap energy, by which the optical responses in the visible-light region are induced.

References

[1] M.A. Fox, M.T. Dulay, Chem. Rev. 93 (1993) 341.
[2] M. Anpo, Y. Ichihashi, M. Takeuchi, H. Yamashita, Res. Chem. Intermed. 24 (1998) 143.
[3] R. Asahi, T. Morikawa, T. Ohwaki, K. Aoki, Y. Taga, Science 293 (2001) 269.
[4] T. Yamaki, T. Sumita, S. Yamamoto, J. Mater. Sci. Lett. 21 (2002) 33.
[5] J.F. Ziegler, J.P. Biersack, U. Littmack, The Stopping Range of Ions in Solids, Pergamon Press, New York, 1985.
[6] G.P. Pells, Radiat. Eff. 64 (1982) 71.
[7] E. Wimmer, H. Krakauer, M. Weinert, A.J. Freeman, Phys. Rev. B 24 (1981) 864.
[8] J.P. Perdew, K. Burke, M. Ernzerhof, Phys. Rev. Lett. 77 (1996) 3856.
[9] T. Umebayashi, T. Yamaki, H. Itoh, K. Asai, J. Phys. Chem. Solids 63 (2002) 1909.
[10] R. Fromknecht, I. Khubeis, S. Massing, O. Meyer, Nucl. Instr. and Meth. B 147 (1999) 191 and references therein.
[11] J. Gebauer, S. Eichler, R. Krause-Rehberg, H.P. Zeindl, Appl. Surf. Sci. 116 (1997) 247.
[12] A. van Veen, H. Schut, M. Clement, J.M.M. de Nijs, A. Kruseman, M.R. Ijpma, Appl. Surf. Sci. 85 (1995) 216.
[13] L.S. Darken, R.W. Gurry, Physical Chemistry of Metals, McGraw Hill, New York, 1953.
[14] J. Senzaki, K. Fukuda, S. Imai, Y. Tanaka, N. Kobayashi, H. Tanoue, H. Okoshi, K. Arai, Appl. Surf. Sci. 159–160 (2000) 544.
[15] V. Kyllönen, J. Räisänen, A. Seppälä, T. Ahlgren, J. Likonen, Nucl. Instr. and Meth. B 161–163 (2000) 673.
[16] D.C. Cronemeyer, Phys. Rev. 113 (1959) 1222.
[17] I. Nakamura, N. Negishi, S. Kutsuna, T. Ihara, S. Sugihara, K. Takeuchi, J. Mol. Catal. A: Chem. 161 (2000) 205.